Quantum chaos in ultracold collisions between Yb($^1S_0$) and Yb($^3P_2$)

Dermot G. Green,* Christophe L. Vaillant,† Matthew D. Frye, Masato Morita, and Jeremy M. Hutson‡
Joint Quantum Centre (JQC) Durham-Newcastle, Department of Chemistry, Durham University, South Road, Durham, DH1 3LE, United Kingdom

(Received 23 October 2015; published 4 February 2016)

We calculate and analyze Feshbach resonance spectra for ultracold Yb($^1S_0$) + Yb($^3P_2$) collisions as a function of an interatomic potential scaling factor λ and external magnetic field. We show that, at zero field, the resonances are distributed randomly in λ, but that signatures of quantum chaos emerge as a field is applied. The random zero-field distribution arises from superposition of structured spectra associated with individual total angular momenta. In addition, we show that the resonances with respect to magnetic field in the experimentally accessible range of 400 to 2000 G are chaotically distributed, with strong level repulsion that is characteristic of quantum chaos.

DOI: 10.1103/PhysRevA.93.022703

I. INTRODUCTION

Ultracold collisions involving the lanthanides Er and Dy in magnetic fields exhibit dense Feshbach resonance spectra that show strong signatures of quantum chaos [1–3]. The density of the spectra results from large reduced masses that produce a large number of bound levels. The complexity arises from anisotropic interactions, which couple different end-over-end angular momenta of the colliding pair [4,5], combined with magnetic fields, which couple different total angular momenta. Chaotic behavior is likely to make the assignment of quantum numbers to individual resonances and prediction of their positions impossible. However, spectra of this type are amenable to statistical analysis [6] that can yield physical insight on the system [7], identifying the presence of good quantum numbers or strong mixing.

Statistical analysis of complex spectra and sets of levels has been applied to a plethora of physical systems. These include nuclear energy levels [8], spectra of complex atoms [9,10] and ions [11], and Rydberg spectra of hydrogen atoms in large magnetic fields [12]. The statistics that are most commonly studied include the distribution of nearest-neighbor level spacings and the level-number variance [7,13]. The nearest-neighbor spacing (NNS) distribution of a randomly distributed set of levels is of Poisson type, while that of a chaotically distributed set is of Wigner–Dyson type. The Wigner–Dyson distribution exhibits strong level repulsion, i.e., vanishingly small probabilities of finding levels that coincide. The Feshbach resonance spectra for Er + Er and Dy + Dy show statistics that indicate a considerable degree of chaos [1,2,14], which for Dy increases steadily with magnetic field [2].

The appearance of chaos in ultracold collision systems has important consequences for their properties. Chaos implies full redistribution of energy between all degrees of freedom. It is likely to result in long-lived two-body collisions, which in turn can produce three-body losses [15]. It is therefore very important to delineate the circumstances in which chaos arises. Er + Er and Dy + Dy are very complex systems involving many different electronic states. By contrast, ultracold collisions in the simpler system Li + Er [16] have recently been shown *not* to exhibit chaos. In this paper, we calculate and analyze the spectrum of Feshbach resonance positions in ultracold collisions between bosonic ground-state Yb($^1S_0$) and metastable Yb($^3P_2$) ytterbium atoms. We show that, even in this remarkably simple system, application of a magnetic field induces a transition to strongly chaotic statistics.

Yb($^1S_0$) + Yb($^3P_2$) is of interest for applications in quantum information processing [17] and quantum computing [18,19]. Takahashi and coworkers have measured Feshbach resonances in this system [20,21], and we discuss how the signatures of quantum chaos could be observed with current experimental capabilities.

II. CALCULATION OF NEAR-THRESHOLD BOUND STATES

Yb($^1S_0$) + Yb($^3P_2$) is a particularly simple case of atom-atom interactions with strong anisotropy. In a spin-orbit-free representation, there are only four electronic states arising from the interaction, of which two ($^3\Sigma_g$ and $^3\Pi_g$) contribute to s-wave scattering. When spin-orbit coupling is included, there are three Born–Oppenheimer curves that correlate with the $^1S_0 + {}^3P_2$ threshold. This contrasts with 49 and 81 curves for the $^3H_6$ and $^5I_8$ states of the submerged f-shell atoms Er and Dy.

Zero-energy Feshbach resonances occur when bound or quasibound states cross the energy threshold of the entrance channel as a function of a parameter such as magnetic field [22]. In this work we perform coupled-channel calculations to obtain the positions of near-threshold bound levels as a function of either magnetic field B or a constant λ that scales the interatomic interaction potential $V \to \lambda V$. Such a potential scaling factor, previously used to explore the sensitivity of coupled-channel calculations to uncertainties in the potential [23–25], is used here to sample different Hamiltonians while retaining a realistic model of the system.

We solve the Schrödinger equation for bound states or scattering in coupled-channel form. We use the atom-atom

*Present address: Centre for Theoretical Atomic, Molecular and Optical Physics, School of Mathematics and Physics, Queen's University Belfast, Belfast BT7 1NN, Northern Ireland, United Kingdom; d.green@qub.ac.uk
†c.l.j.j.vaillant@durham.ac.uk
‡j.m.hutson@durham.ac.uk

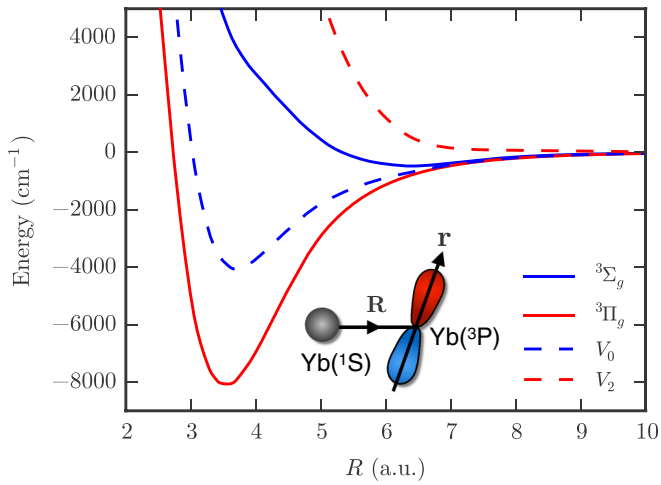

FIG. 1. Interatomic potentials for Yb(^1S) + Yb(^3P). Σ and Π Born–Oppenheimer potentials calculated from Ref. [29] (red lines). Isotropic $V_0(R)$ and anisotropic $V_2(R)$ Legendre expansion coefficients, as described in the text (blue lines).

Hamiltonian described in Ref. [26], except that in the present case Yb(^3P_j) interacts with a structureless partner. The interaction potential $\hat{V}$ can be written as the Legendre expansion $\hat{V}(\mathbf{R},\hat{\mathbf{r}}) = \sum_{k=0,2} V_k(R)P_k(\hat{\mathbf{R}}\cdot\hat{\mathbf{r}})$ [4,27], where $\mathbf{R}$ is the internuclear separation vector and $\hat{\mathbf{r}}$ is a unit vector describing the position of the Yb $6p$ electron. The expansion coefficients are $V_0 = (V_\Sigma + 2V_\Pi)/3$ and $V_2 = 5(V_\Sigma - V_\Pi)/3$ [5,28], where V_Σ and V_Π are the $^3\Sigma_g$ and $^3\Pi_g$ Born–Oppenheimer potentials. Figure 1 shows the $^3\Sigma_g$ and $^3\Pi_g$ potentials of Ref. [29], together with V_0 and V_2. Physically, the anisotropy is due to the $6p$ valence electron of [Xe]$4f^{14}6s6p$Yb(^3P). As a result, the anisotropy in this system is much larger than in the Er + Er and Dy + Dy systems, which involve f-shell electrons submerged beneath a closed $6s$ shell [1,2]. We extrapolate the potentials at long range with the dispersion form $-C_6/R^6$ [30], using calculated dispersion coefficients of 2999 and $2649 E_h a_0^6$ [31] for the $^3\Sigma_g$ and $^3\Pi_g$ states, respectively. The spin-orbit interaction is taken to be independent of $\mathbf{R}$, with a coupling constant that gives the correct splitting between the $^3P_2$ and $^3P_1$ states [32].

At zero field the total angular momentum is a good quantum number due to the isotropy of free space. In the absence of a field, we use the space-fixed total angular momentum basis set $|(ls)jLJM_J\rangle$ [4]. Here the atomic orbital and spin angular momenta l and s couple to give a resultant j, which then couples to the end-over-end angular momentum L to give the total angular momentum J. At finite magnetic field we use the partially uncoupled basis set $|(ls)jm_jLM_L\rangle$, where m_j and M_L are the projections of j and L onto the field axis, respectively [26]. We include values of L up to $L_{\max} = 22$, for which the pattern of the Feshbach resonance spectrum is converged. Increasing the value of $L_{\max}$ introduces additional bound states, but they are very weakly coupled to the entrance channel.

The coupled equations for atom-atom scattering are solved using the MOLSCAT package [33], modified to handle magnetic fields [34] and P-state atoms [26]. Bound states are located using the FIELD package [35], which solves the coupled-channel equations subject to bound-state boundary conditions by using the methods of Ref. [36] to locate the magnetic fields at which bound states exist with a specified binding energy.

In this work, we consider resonances in s-wave collisions of Yb($^3P_2$) in its $m_j = -2$ state. This is the lowest component of the $j = 2$ manifold. Inelastic decays to the $j = 0$ and $j = 1$ manifolds in two-body collisions with Yb(^1S) are slow, with a decay rate that has been measured to have an upper bound of 10^{-13} cm^3/s at fields below 1 G [37]. We performed coupled-channel calculations of the inelastic rate over the range 0 to 2000 G and find the background rate to be significantly smaller than this bound, on the order of 10^{-17} cm^3/s. The slow two-body decay makes experiments on three-body losses in this system viable.

Using the FIELD package at the energy of the lowest threshold produces a list of fields at which zero-energy Feshbach resonances occur [38]. For the present work we extended the FIELD package to converge on levels (and thus resonance positions) as a function of potential scaling factor λ as well as magnetic field. In order to locate resonances at the $j = 2$, $m_j = -2$ threshold, basis functions for $j = 0$ and 1 were omitted, corresponding to neglect of the slow inelastic decays considered above. We expect this approximation to have no significant effect on level statistics.

III. STATISTICAL ANALYSIS

We analyze sets of levels (or resonance positions) through two commonly used statistics: the nearest-neighbor spacing (NNS) distribution, which is the probability density $P(s)$ of two neighboring levels having the spacing s, and the variance in the number of levels in a given energy range. These statistics probe short-range correlations (on the order of a few mean level spacings) and longer-range correlations, respectively [7,13].

The NNS distribution and number variance must be calculated from a set of levels on a dimensionless scale with unit local number density: the "unfolded" scale. To obtain the unfolded levels from the calculated levels X_i, we first construct the staircase function $S(X) = \sum_i \Theta(X - X_i)$, where Θ is the Heaviside function. X is commonly the energy but here is either B or λ. We then fit a low-order polynomial $\xi(X)$ to the smoothly varying average density, isolating the fluctuations that are of interest, and obtain the unfolded levels ξ_i by mapping $X_i \to \xi_i = \xi(X_i)$ [7].[1]

The NNS distribution is commonly used to distinguish between regular and chaotic systems. For an uncorrelated (random) spectrum, the NNSs on the unfolded scale $s_i = \xi_{i+1} - \xi_i$ are distributed according to Poisson statistics $P_P(s) = \exp(-s)$

[1]In general, $S(X)$ can be decomposed as $S(X) = \xi(X) + S_{\rm fl}(X)$, where $\xi(X)$ is a smooth part given by the cumulative mean level density, and $S_{\rm fl}(X)$ describes fluctuations about this average. The unfolding procedure rescales the staircase function $S(X) \to S(\xi) = \xi + S_{\rm fl}(\xi)$, i.e., to unit average density, isolating the fluctuating part that is of interest.

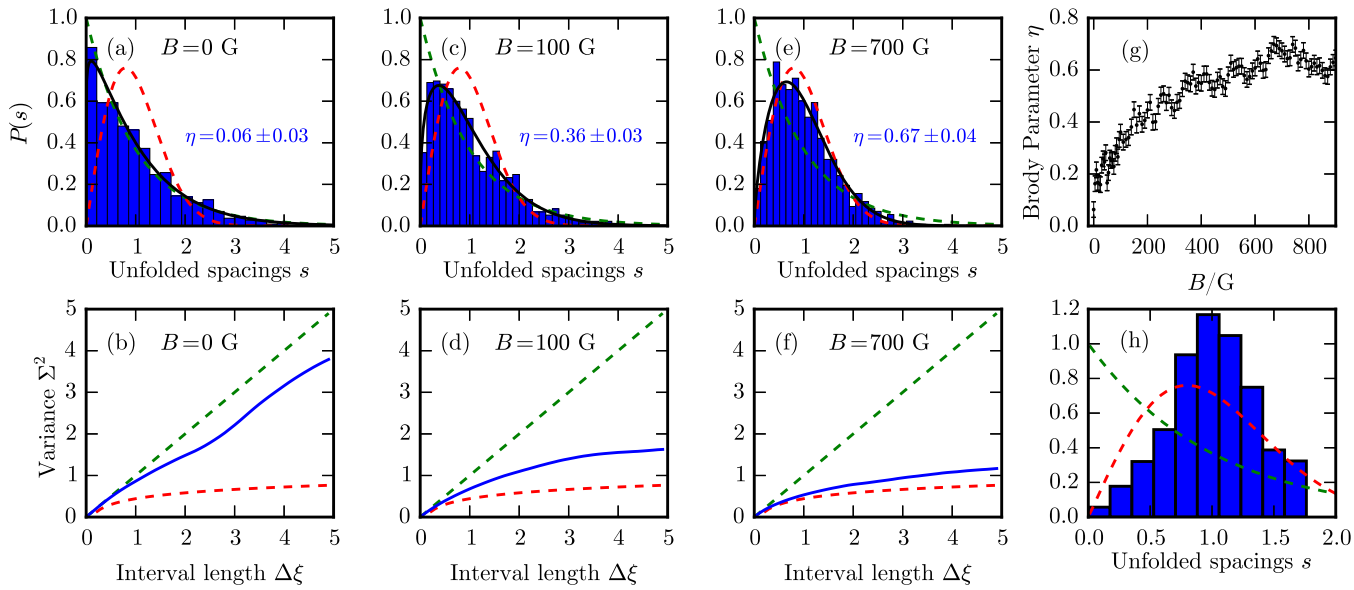

FIG. 2. Statistical analysis of Feshbach resonance positions with respect to potential scaling factor λ. Panels (a), (c), and (e) show the NNS distributions $P(s)$: coupled-channel results (blue histograms); fitted Brody distributions (black lines, with the corresponding Brody parameters stated); Poisson and Wigner–Dyson distributions (green and red dashed lines, respectively). Panels (b), (d), and (f) show the corresponding number variances $\Sigma^2(\Delta\xi)$: coupled-channel results (blue solid lines); Poisson and GOE results (green and red dashed lines, respectively). (g) Calculated Brody parameter as a function of magnetic field. (h) NNS distribution for individual blocks of total angular momentum J in the absence of magnetic field, averaged over $J = 2,\ldots,20$.

[7,13]. By contrast, for a chaotic system the distribution is well approximated by the Wigner–Dyson form $P_{\mathrm{WD}}(s) = (\pi s/2)\exp(-\pi s^2/4)$ [7,13], with strong level repulsion. This distribution is an approximation to the prediction of the Gaussian orthogonal ensemble (GOE) [7], which the Bohigas–Giannoni–Schmit conjecture [39] suggests is the appropriate random-matrix-theory model for a quantum system that is chaotic in the classical limit.

Physical systems rarely conform to either of these special cases. Following recent practice in the cold-matter literature [1,2,40], we interpolate between the Poisson and Wigner–Dyson cases by using the Brody ansatz $P_{\mathrm{B}}^{(\eta)}(s) = c_\eta(1+\eta)s^\eta \exp(-c_\eta s^{\eta+1})$, where $c_\eta = \Gamma[(\eta+2)/(\eta+1)]^{\eta+1}$ [41]. We note that other methods of interpolating between the Poisson and Wigner–Dyson NNS distributions exist, including rigorous semiclassical expressions [42]. The "Brody parameter" η takes values between zero (Poisson distribution) and unity (Wigner–Dyson distribution). We calculate η by maximum likelihood estimation [43], maximizing the log-likelihood function $l(\eta) = \sum_i \ln P_{\mathrm{B}}^{(\eta)}(s_i)$ with respect to η. The uncertainty in η is thus the standard deviation $\sigma = (-d^2 l/d\eta^2)^{-1/2}$.

The second statistic that we consider, to probe long-range correlations, is the level-number variance Σ^2. This is defined as $\Sigma^2(\Delta\xi) = \langle \hat{S}^2(\Delta\xi,\xi)\rangle - \langle \hat{S}(\Delta\xi,\xi)\rangle^2$, where $\hat{S}(\Delta\xi,\xi)$ counts the number of levels in the interval $[\xi,\xi+\Delta\xi]$ and the average is taken over the starting values ξ [7,13]. For a randomly distributed (Poisson) set it is $\Sigma^2(\Delta\xi) = \Delta\xi$, whereas for a Hamiltonian belonging to the GOE it is $\Sigma^2(\Delta\xi) = 2\pi^{-2}[\ln(2\pi\Delta\xi) + \gamma + 1 - \pi^2/8] + O(\Delta\xi^{-1})$, where $\gamma = 0.5772\ldots$ is Euler's constant [7,13].

IV. RESULTS AND DISCUSSION

Figures 2(a)–2(f) show the NNS distribution and number variance for a sequence of 1000 resonance positions calculated with respect to λ on the range [0.9,1.13] and in external magnetic fields of 0, 100, and 700 G. In the absence of a field, the NNS distribution and the number variance are close to those expected for Poisson statistics, with a Brody parameter $\eta = 0.06 \pm 0.03$. However, application of a magnetic field induces a clear transition towards chaotic statistics. Figure 2(g) shows the Brody parameter η as a function of field B: it rises steadily from close to zero at $B = 0$ to a value around 0.6 at fields above 500 G. The high-field value is comparable to that observed experimentally for Er and Dy [2]. The number variance also changes steadily from near-Poissonian to chaotic behavior as the field increases, following the GOE prediction at high field more strongly than for Er and Dy.

Let us consider further the result at zero field, where the total angular momentum J is a good quantum number. In Fig. 2(h) we show the NNS distribution for individual Hamiltonian blocks of a given total angular momentum J, averaged over values of $J = 2,\ldots,20$ to obtain improved statistics.[2] Although this superficially resembles a Wigner–Dyson distribution, except that there is a cutoff at large spacing, the levels associated with individual blocks of the total Hamiltonian are in fact highly structured. They correspond to

[2]The average is performed by first calculating the unfolded spacings for each J before combining the sets and normalizing the resulting histogram.

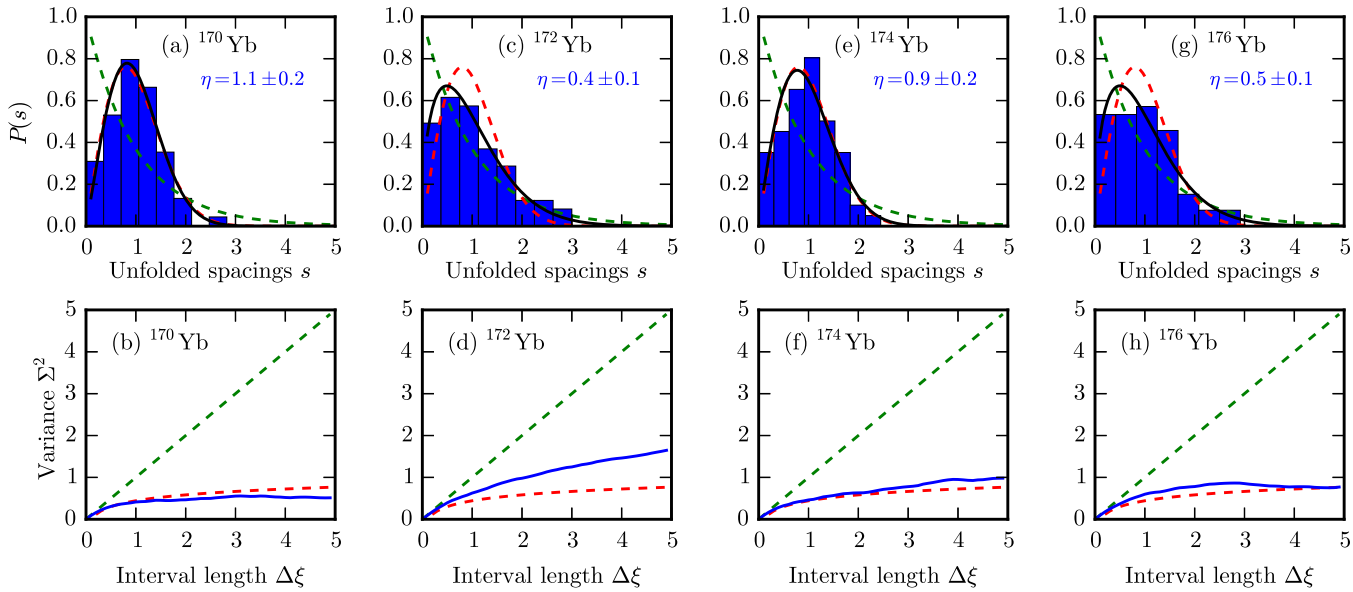

FIG. 3. Statistical analysis of Feshbach resonance positions with respect to magnetic field for different isotopes of Yb. Upper panels show NNS distributions $P(s)$: coupled-channel calculations (blue histograms); fitted Brody distributions (black lines, with the corresponding Brody parameters stated); Poisson and Wigner–Dyson distributions (green and red dashed lines, respectively). Lower panels show the corresponding number variances $\Sigma^2(\Delta\xi)$: coupled-channel calculations (blue solid lines); Poisson and GOE results (green and red dashed lines, respectively).

the superposition of nearly independent sequences for $|\Omega| = 0$, 1, and 2, where Ω is the projection of J onto the interatomic axis.[3] It is evident that the Poisson statistics exhibited by the full spectrum at zero field result from superposition of these structured spectra.

Thus far we have considered the distribution of resonances with respect to an interatomic potential scaling factor. We now consider the distribution of Feshbach resonances with respect to magnetic field, for homonuclear collisions involving the four most abundant bosonic isotopes of Yb. The typical density of resonances is $\sim$0.05 G^{-1}. This is comparable to that found in Cs [44] and Li + Er [16], but less than that observed in the Er and Dy systems, where it can be as large as $\sim$4G^{-1} (for bosonic isotopes) [1,2].

Figure 3 shows the NNS distributions and number variances for ^{170}Yb, ^{172}Yb, ^{174}Yb, and ^{176}Yb in the field range of 400 to 2000 G. The statistics show strong signatures of chaos in each case, with Brody parameters ranging from 0.4 to about 1 and number variances much closer to the GOE predictions than to Poisson statistics. We emphasize that the statistics depend on the potential scaling factor as well as on the isotopic mass, so the results in Fig. 3 are representative of typical behavior, rather than specific predictions for individual isotopes. Signatures of chaos emerge at somewhat different fields for different cases but are always strongly present for fields over 600 G. These signatures will be observable if current experiments on Feshbach resonances in Yb($^1S_0$) + Yb($^3P_2$) [20,21] can be extended to suitable magnetic fields.

[3]The cutoff at approximately $s = 1.8$ in Fig. 2(h) is consistent with the vibrational spacing for the $|\Omega| = 2$ potential at dissociation, calculated with respect to λ. This is the deepest of the three potentials and is equivalent to the $^3\Pi_g$ potential.

The results in Figs. 2 and 3 show that a large number of electronic states is not required for signatures of chaos to emerge in ultracold collisions, as may have been expected from the Er and Dy examples. We conclude that chaos in Yb + Yb* emerges as a result of the combination of strongly anisotropic interactions and magnetic field, consistent with the findings for Dy + Dy [2]. As a counterexample, we analyzed the Feshbach resonance positions in Cs(^2S) + Cs(^2S) collisions in magnetic field [44], where there are two electronic states but only very weak anisotropy. We find no deviations from Poisson statistics for Cs.

V. CONCLUSIONS

We have calculated and statistically analyzed the positions of Feshbach resonances for collisions of ground-state and metastable Yb. This is one of the simplest possible cases of atom-atom interactions with strong anisotropy. Even in this remarkably simple system, the application of an external magnetic field induces a transition from random (Poisson) statistics at zero field to chaotic statistics at high field. This suggests that chaos is likely to be widespread in ultracold collisions, which will have important consequences for the lifetimes of ultracold species. We predict that the positions of magnetically tunable Feshbach resonances for the four most abundant bosonic Yb isotopes will exhibit strong signatures of quantum chaos at high magnetic fields. These signatures could be observed in experiments within reach of current technology.

The data presented in this paper are available online [45].

ACKNOWLEDGMENTS

The authors thank C. Ruth Le Sueur, Maykel L. González-Martínez, and Paul S. Julienne for valuable discussions. This work was supported by the Engineering and Physical Sciences Research Council under Grant No. EP/I012044/1.

[1] A. Frisch, M. Mark, K. Aikawa, F. Ferlaino, J. L. Bohn, C. Makrides, A. Petrov, and S. Kotochigova, Nature (London) **507**, 475 (2014).

[2] T. Maier, H. Kadau, M. Schmitt, M. Wenzel, I. Ferrier-Barbut, T. Pfau, A. Frisch, S. Baier, K. Aikawa, L. Chomaz, M. J. Mark, F. Ferlaino, C. Makrides, E. Tiesinga, A. Petrov, and S. Kotochigova, Phys. Rev. X **5**, 041029 (2015).

[3] T. Maier, I. Ferrier-Barbut, H. Kadau, M. Schmitt, M. Wenzel, C. Wink, T. Pfau, K. Jachymski, and P. S. Julienne, Phys. Rev. A **92**, 060702 (2015).

[4] R. H. G. Reid and A. Dalgarno, Phys. Rev. Lett. **22**, 1029 (1969).

[5] R. V. Krems, G. C. Groenenboom, and A. Dalgarno, J. Phys. Chem. A **108**, 8941 (2004).

[6] E. P. Wigner, Math. Proc. Cambridge Philos. Soc. **47**, 790 (1951).

[7] T. Guhr, A. Müller-Groeling, and H. A. Weidenmüller, Phys. Rep. **299**, 189 (1998).

[8] T. A. Brody, J. Flores, J. B. French, P. A. Mellow, A. Pandey, and S. S. M. Wong, Rev. Mod. Phys. **53**, 385 (1981).

[9] N. Rosenzweig and C. E. Porter, Phys. Rev. **120**, 1698 (1960).

[10] V. V. Flambaum, A. A. Gribakina, G. F. Gribakin, and M. G. Kozlov, Phys. Rev. A **50**, 267 (1994).

[11] V. V. Flambaum, M. G. Kozlov, and G. F. Gribakin, Phys. Rev. A **91**, 052704 (2015).

[12] H. Friedrich and H. Wintgen, Phys. Rep. **183**, 37 (1989).

[13] M. L. Mehta, *Random Matrices*, 2nd ed. (Academic Press, San Diego, 1991).

[14] J. Mur-Petit and R. A. Molina, Phys. Rev. E **92**, 042906 (2015).

[15] M. Mayle, B. P. Ruzic, and J. L. Bohn, Phys. Rev. A **85**, 062712 (2012).

[16] M. L. González-Martínez and P. S. Żuchowski, Phys. Rev. A **92**, 022708 (2015).

[17] A. V. Gorshkov, A. M. Rey, A. J. Daley, M. M. Boyd, J. Ye, P. Zoller, and M. D. Lukin, Phys. Rev. Lett. **102**, 110503 (2009).

[18] K. Shibata, S. Kato, A. Yamaguchi, S. Uetake, and Y. Takahashi, Appl. Phys. B: Lasers Opt. **97**, 753 (2009).

[19] A. J. Daley, M. M. Boyd, J. Ye, and P. Zoller, Phys. Rev. Lett. **101**, 170504 (2008).

[20] S. Kato, S. Sugawa, K. Shibata, R. Yamamoto, and Y. Takahashi, Phys. Rev. Lett. **110**, 173201 (2013).

[21] S. Taie, S. Watanabe, T. Ichinose, and Y. Takahashi, Phys. Rev. Lett. **116**, 043202 (2016).

[22] C. Chin, R. Grimm, E. Tiesinga, and P. S. Julienne, Rev. Mod. Phys. **82**, 1225 (2010).

[23] M. T. Cvitaš, P. Soldán, J. M. Hutson, P. Honvault, and J. M. Launay, J. Chem. Phys. **127**, 074302 (2007).

[24] A. O. G. Wallis and J. M. Hutson, Phys. Rev. Lett. **103**, 183201 (2009).

[25] A. O. G. Wallis, E. J. J. Longdon, P. S. Żuchowski, and J. M. Hutson, Eur. Phys. J. D **65**, 151 (2011).

[26] M. L. González-Martínez and J. M. Hutson, Phys. Rev. A **88**, 020701R (2013).

[27] J. Callaway and E. Bauer, Phys. Rev. **140**, A1072 (1965).

[28] V. Aquilanti and G. Grossi, J. Chem. Phys. **73**, 1165 (1980).

[29] Y. X. Wang and M. Dolg, Theor. Chem. Acta **100**, 124 (1998).

[30] A. J. Stone, *The Theory of Intermolecular Forces* (Oxford University Press, Oxford, 1996).

[31] S. G. Porsev, M. S. Safronova, A. Derevianko, and C. W. Clark, Phys. Rev. A **89**, 012711 (2014).

[32] W. F. Meggers and J. L. Tech, J. Res. Natl. Bur. Stand. **83**, 13 (1978).

[33] J. M. Hutson and S. Green, MOLSCAT Computer Program, Version 14, distributed by Collaborative Computational Project No. 6 of the UK Engineering and Physical Sciences Research Council (1994).

[34] M. L. González-Martínez and J. M. Hutson, Phys. Rev. A **75**, 022702 (2007).

[35] J. M. Hutson, FIELD Computer Program, Version 1 (2011).

[36] J. M. Hutson, Comput. Phys. Commun. **84**, 1 (1994).

[37] S. Uetake, R. Murakami, J. M. Doyle, and Y. Takahashi, Phys. Rev. A **86**, 032712 (2012).

[38] Y. V. Suleimanov and R. V. Krems, J. Chem. Phys. **134**, 014101 (2011).

[39] O. Bohigas, M. J. Giannoni, and C. Schmit, Phys. Rev. Lett. **52**, 1 (1984).

[40] K. Jachymski and P. S. Julienne, Phys. Rev. A **92**, 020702 (2015).

[41] T. Brody, Lett. Nuovo Cimento **7**, 482 (1973).

[42] M. V. Berry and M. Robnik, J. Phys. A: Math. Gen. **17**, 2413 (1984).

[43] R. J. Barlow, *Statistics: A Guide to the Use of Statistical Methods in the Physical Sciences* (Wiley, Chichester, 1989).

[44] M. Berninger, A. Zenesini, B. Huang, W. Harm, H.-C. Nägerl, F. Ferlaino, R. Grimm, P. S. Julienne, and J. M. Hutson, Phys. Rev. A **87**, 032517 (2013).

[45] D. G. Green, C. L. Vaillant, M. D. Frye, M. Morita, and J. M. Hutson, doi:10.15128/ns0646000 (2015).